Journal of Nuclear Medicine, published on March 9, 2018 as doi:10.2967/jnumed.118.208009

Evaluation of ^{11}C-BU99008, a positron emission tomography ligand for the Imidazoline$_2$ binding site in human brain

Robin J. Tyacke[1], Jim F.M. Myers[1], Ashwin Venkataraman[1], Inge Mick[1], Samuel Turton[1], Jan Passchier[3], Stephen M. Husbands[4], Eugenii A. Rabiner[3], Roger N. Gunn[2,3], Philip S. Murphy[5], Christine A. Parker[1,5] and David J. Nutt[1].

[1]Neuropsychopharmacology Unit, Centre for Academic Psychiatry, Division of Brain Sciences, Imperial College London, Burlington Danes Building, Hammersmith Hospital campus, 160 Du Cane Road, London W12 0NN

[2]Restorative Neurosciences, Imperial College London, Burlington Danes Building, Hammersmith Hospital campus, 160 Du Cane Road, London W12 0NN

[3]Imanova Limited, Burlington Danes Building, Imperial College London, Hammersmith Hospital, Du Cane Road, London, W12 0NN

[4]Department of Pharmacy and Pharmacology, University of Bath, Claverton Down, Bath BA2 7AY

[5]Experimental Medicine Imaging, GlaxoSmithKline Research & Development Limited, Gunnels Wood Road, Stevenage, SG1 2NY

Corresponding Author: R Tyacke, Centre for Neuropsychopharmacology, Imperial College London, Burlington Danes Building, Hammersmith Hospital campus, 160 Du Cane Road, London W12 0NN, t: 020 7594 7096, f: 020 7594 6548, e: r.tyacke@imperial.ac.uk

WORD COUNT: 4572

RUNNING TITLE: ^{11}C-BU99008 binding in Humans

ABSTRACT

The imidazoline$_2$ binding sites (I_2BS), are thought to be expressed in glia, and implicated in the regulation of glial fibrillary acidic protein. A positron emission tomography (PET) ligand for this target would be important for the investigation of neurodegenerative and neuroinflammatory diseases. ^{11}C-BU99008 has previously been identified as a putative PET radioligand. Here we present the first *in vivo* characterisation of this PET radioligand in humans and assess its test-retest reproducibility. **Methods:** 14 healthy male volunteers underwent dynamic PET imaging with ^{11}C-BU99008 and arterial sampling. Six subjects were used to assess test-retest and eight were used in the pharmacological evaluation, undergoing a second, or third heterologous competition scan with the mixed I_2BS/α_2-adrenoceptor drug, idazoxan (n=8; 20, 40, 60 and 80 mg) and the mixed irreversible monoamine oxidase (MAO) A/B inhibitor, isocarboxazid (n=4; 50 mg), respectively. Regional time-activity data were generated from arterial plasma input functions corrected for metabolites using the most appropriate model to derive the outcome measure V_T (regional total distribution volume). All image processing and kinetic analysis was performed in MIAKAT™ (www.miakat.org). **Results:** Brain uptake of ^{11}C-BU99008 was good with reversible kinetics and a heterogeneous distribution consistent with known I_2BS expression. Model selection criteria indicated that the 2-tissue-compartment was preferred. V_T estimates were high in the striatum (105±21 mL·cm^{-3}), medium in cingulate cortex (62±10 mL·cm^{-3}) and low in the cerebellum (41±7 mL·cm^{-3}). Test-retest reliability was found to be reasonable. The uptake was dose-dependently reduced by pre-treatment with idazoxan throughout the brain, with an average block across all regions of ~60% (V_T≅30 mL·cm^{-3}) at the highest dose (80 mg). The median effective dose (ED_{50}) for idazoxan was calculated as 28 mg. Uptake was not blocked by pre-treatment with the MAO inhibitor, isocarboxazid. **Conclusions:** In summary, ^{11}C-BU99008 in human PET studies demonstrates good brain delivery, reversible kinetics, heterogeneous distribution specific binding signal consistent with I_2BS distribution and good test-retest reliability.

Keywords: ^{11}C-BU99008, Imidazoline$_2$ binding site, I_2BS, positron emission tomography, PET, BU99008

INTRODUCTION

The ability of the α_2-adrenoceptor agonist clonidine and the antagonist idazoxan, to label a sub-population of binding sites that were not displaceable by the endogenous ligand noradrenaline, led to the discovery of the imidazoline binding sites (IBS) some 25 years ago (*1*). These binding sites have subsequently been divided into three groups: the imidazoline$_1$ binding site (I_1BS) that is preferentially labelled by ^{3}H-clonidine, the imidazoline$_2$ binding site (I_2BS) that is preferentially labelled by ^{3}H-idazoxan, and the imidazoline$_3$ binding site (I_3BS) which is an atypical imidazoline site found on pancreatic β-cells (*2*).

Changes in post-mortem binding density of the I_2BS have implicated them in a range of psychiatric conditions such as depression (*3,4*) and addiction (*5*), along with neurodegenerative disorders such as Alzheimer's disease (*6*) and Huntington's chorea (*7*). Functional interactions in preclinical models have also been shown in relation to the opioid system, where I_2BS ligands have been shown to affect tolerance to morphine (*8,9*) and alleviate elements of the morphine withdrawal syndrome in rats (*10*). The location of I_2BS on glia and the possibility that they may in some way regulate glial fibrillary acidic protein (*11,12*) has led to increased interest into the role of I_2BS and I_2BS ligands in conditions characterised by marked gliosis. The density of I_2BS has been shown to increase in Alzheimer's disease *post mortem* (*6*), and it has also been suggested that I_2BS may be a marker for human glioblastomas (*13*) and that in these tumours the increase seen in I_2BS B_{MAX} was correlated with the severity and malignancy of the glioma (*14*). Subsequent work added weight to this argument showing that the density of I_2BS is increased *in vivo* with heat-induced gliosis (*15*).

Positron emission tomography (PET) is an *in vivo* imaging technique that uses radioligands as selective molecular probes to map the location and density of specific proteins. The development of a selective I_2BS PET radioligand would allow for the characterisation of I_2BS *in vivo* and their regulation in disease states. A number of ligands selective for I_2BS have been reported (*16*), but only two potential PET radioligands

have been reported to date: ^{11}C-benazoline has been synthesised (*17*) but not evaluated *in vivo*, and ^{11}C-FTIMD appears to have low specific signal in rat and primate brain (*18,19*).

We have previously identified and evaluated ^{11}C-BU99008 as a putative I_2BS PET ligand in preclinical species (*20-22*). We have also shown that ^{11}C-BU99008 binds with a significantly lower affinity to monoamine oxidase type B (MAO_B) and thus is selective for I_2BS in these preclinical species. In order to meet the aims of this study and determine the regional density and distribution of I_2BS in healthy human brain, scans using ^{11}C-BU99008 were conducted in the presence and absence of two drugs, idazoxan and isocarboxazid.

Idazoxan is an α_2-adrenoceptor antagonist drug originally investigated in humans for its potential to treat psychiatric conditions (*23,24*). Defined as one of the archetypal I_2BS ligands, idazoxan has a high affinity for the I_2BS with an equilibrium dissociation constant (K_D) of 20nM and 13nM in human cortical (*25*) and striatal (*26*) slices respectively. Isocarboxazid is an irreversible, non-selective MAO inhibitor that has been in use for over 60 years, and is well tolerated in humans (*27*). While there is evidence that some I_2BS ligands also bind to MAO (*28*), ^{11}C-BU99008 shows very low affinity for MAO but still it is essential to know the contribution, if any, of a MAO specific signal. Isocarboxazid was chosen as it will block both isoforms of MAO and has the lowest affinity for I_2BS of the available irreversible non-selective MAO inhibitors (*29*) so minimising any signal confounds.

We present the first *in vivo* evaluation and characterisation of this ligand in healthy human volunteers using competition experiments to determine ^{11}C-BU99008 specificity and selectivity and assess its test-retest reproducibility.

MATERIALS AND METHODS

Radiochemistry

^{11}C-BU99008 was prepared by *N*-alkylation of the desmethyl precursor BU99007 using ^{11}C-CH_3I as previously described (*20,21*) (Supplemental Fig. 1). The final formulation of the ^{11}C-BU99008 was in 20% EtOH/saline solution affording a formulated i.v. preparation ready for dispensing and injection. Checks of chemical and radiochemical purity were performed as well as analysis of the radiochemical yield and molar activity.

Blood and Metabolite analysis

Analysis of ^{11}C-BU99008 metabolism in plasma was performed for each scan as follows: arterial blood samples were collected at 5, 10, 15, 20, 25, 30, 40, 50, 60, 70, 80 and 100 min following ^{11}C-BU99008 injection. Plasma samples were prepared and the fraction of unchanged radioligand was determined using HPLC by the integration of the radioactivity peak corresponding to ^{11}C-BU99008 (retention time ~6.5 min) and expressed as percentage of all the radioactive peaks observed. The final plasma input function was calculated as the product of the total plasma curve and the parent fraction curve.

The free fraction of ^{11}C-BU99008 in plasma (f_P) was measured through ultrafiltration (Amicon Ultra regenerated cellulose MWCO 30kDa, Millex, Ireland) in triplicate and compared to Tris buffer (0.1 M, pH=7.4) to enable correction for non-specific filter binding.

Subjects

This PET study was performed at Imanova Centre for Imaging Sciences, London, UK. The protocol for this study was approved by the national research ethics service (West London Research Ethics Committee (14/LO/1741)) and the national administration of radioactive substances advisory committee (630/3764/32214), and conducted in accordance with good clinical practice guidelines, all applicable regulatory requirements, and the Code of Ethics of the World Medical Association (Declaration of

Helsinki). All subjects provided written and signed informed consent. The study I2PETHV was registered on the clinical trials database, identifier NCT02323217.

Heterologous competition

Eight healthy male volunteers (age 52±8 years) either underwent two or three PET/CT scans with ^{11}C-BU99008 (120 min; SA=50.6±20.1 GBq·µmol^{-1}; Injected Dose=308 ± 14 MBq; Mass=1.7±1.7 µg), in a fixed-order open-label design. The first scan was a baseline with ^{11}C-BU99008 (n=8). Later that day the volunteers received a second PET/CT scan with ^{11}C-BU99008, 120 min after an oral dose of the mixed I_2BS/α2-adrenoceptor drug, idazoxan (20, 40, 60 and 80 mg; n=2 for each dose). At least 1 week later, four of the eight volunteers received a third PET/CT scan with ^{11}C-BU99008 (n=4), 240 min after an oral dose of the mixed irreversible $MAO_{A/B}$ inhibitor, isocarboxazid (50 mg). Idazoxan was synthesized by Onyx Pharmaceuticals Inc., isocarboxazid was purchased from a pharmaceutical supplier (Supplemental Table 1).

Test re-test reproducibility

Six further healthy male volunteers (age 56±6 years) underwent two PET/CT scans with ^{11}C-BU99008 (120 min; SA=35.3±17.5 GBq·µmol^{-1}; Injected Dose=313.9±11 MBq; Mass=2.9±2.5 µg) at least one week apart to determine the test re-test reproducibility of the radioligand quantification.

In both the specificity and selectivity and test re-test experiments the healthy volunteers' vital signs: Heart Rate, and Blood Pressure were monitored before, during and after each PET/CT scan (Supplemental Table 1).

Magnetic Resonance Imaging

To enable accurate anatomical parcellation of the PET data, each volunteer also underwent a T1-weighted structural magnetic resonance imaging (Magnetom Trio Syngo MR B13 Siemens 3T; Siemens AG, Medical Solutions) for atlas-based region-of-interest (ROI) delineation.

PET imaging

PET scans were acquired for 120 min on a HiRez Biograph 6 PET/CT scanner (Siemens Healthcare, Erlangen, Germany) and reconstructed into 29 frames (8×15, 3×60, 5×120, 5×300, 8×600 s) using filtered back-projection. Dynamic images were corrected for motion using a mutual information co-registration algorithm with frame 16 as the reference. ^{11}C-BU99008 was manufactured at Imanova Centre for Imaging Sciences (London, UK), immediately prior to use according to local standard operating procedures for GMP production, and injected as an intravenous bolus over approximately 20 s and the PET emission data collected. An arterial line was placed in all subjects and blood was sampled continuously for 15 min as well as manually withdrawn discrete blood samples taken at 5, 10, 15, 20, 25, 30, 40, 50, 60, 70, 80, 90, 100, 110 and 120 min following ^{11}C-BU99008 injection. Arterial blood radioactivity could then be converted to a total plasma concentration and corrected by the parent fraction to determine a parent plasma input function. CT data were also collected for attenuation-correction purposes.

Regional time-activity curve sampling and modelling

All image processing and kinetic analysis was performed using MIAKAT™ (www.miakat.org). MRI structural data and PET data were coregistered into a mutual space and the non-linear registration of a standard MNI template to the structural image provided the parameters to warp the CIC atlas (*30*). This permitted the regional sampling of the PET data and generation of motion-corrected time-activity data for selected ROIs.

Parent plasma input functions were derived from the arterial blood measurements, the whole-blood data corrected for plasma and metabolite fractions using sigmoid models, and interpolated with a tri-exponential function. These were used as input functions to one-tissue compartment (1TCM), two-tissue compartment (2TCM) and multilinear analysis (MA1) (*31*) models. The most appropriate model was selected using the Akaike Information Criterion (AIC) as well as percent reliability, calculated using Equation 1. It was found that there was no suitable reference tissue and so the occupancy plot was used to calculate the non-displaceable volume of distribution (V_{ND}) and receptor occupancy (*32*).

EQUATION 1: $$VAR = \frac{100}{N}\sum_{i=1}^{N}\frac{|test_i - retest_i|}{|test_i + retest_i|/2}$$

RESULTS

Radiochemistry

^{11}C-BU99008 was successfully synthesised with a radiochemical purity of 100% at the end of synthesis. The specific activity was 44.8±19 GBq·μmol^{-1} and an average mass of 2.1±2.1 μg and radioactive dose of 310±13.3 MBq was injected for all the synthesis/administrations in this study. The identity of the radiolabelled material was confirmed by co-injection with a sample of authentic BU99008, which, under the same elution conditions, showed an identical retention time. There is a complete table of the ^{11}C-BU99008 parameters in supplemental data (Supplemental Table 1).

Regional time-activity curve computation and Modelling

Brain uptake of ^{11}C-BU99008 was rapid with reversible kinetics and a heterogeneous distribution consistent with known I_2BS expression (*20,21*). The arterial blood samples were used to determine a plasma input function (Fig. 1) to enable modelling of the TACs and estimation of the total volume of

distribution (V_T). The ^{11}C-BU99008 was metabolised such that ~10% of the parent radioligand remained in plasma at 120 min for all scans regardless of intervention.

Comparison of AIC (see Table 1) and assessment of the robustness of fits of the 1TCM and 2TCM models in a selection of ROIs suggested that the 2TCM, with a fixed 5% blood volume, was the most appropriate compartmental model. Test-retest variability (within subject, *VAR*, see Eq. 1) for these ROIs were also compared using 1TCM, 2TCM and MA1, and again 2TCM was the model identified as showing the greatest reliability. As a result, this model was used to derive regional volumes of distribution (V_T) estimates. The robust nature of MA1 suggests it remains a suitable option for a voxel-wise analytical approach with this tracer, and while modulating t* has little effect on the outcome measure, a differing regional underestimation of V_T compared to 2TCM may be noted.

Distribution and heterologous competition

Peak radioactive concentrations were observed approximately 10-20 minutes after administration of ^{11}C-BU99008, followed by a slow washout from all regions (Fig. 2). The uptake was highest in the striatum (V_T=105.7±21.0 ml·cm^{-3}) and lowest in the cerebellum (V_T=41.9±6.9 ml·cm^{-3}) (see Table 1). The regional uptake in humans correlated well to that seen pre-clinically in pig (r=0.71; P<0.05) and primate (r=0.84; P<0.05). ^{11}C-BU99008 V_T was dose dependently reduced by pre-treatment with an oral dose of the mixed I_2BS/α_2-adrenoceptor drug, idazoxan, with an average block across all regions of approximately 60% at the highest dose (80 mg; Figs. 3 and 4). There was no region devoid of blockade, indicating there is no suitable reference tissue for this ligand. Pre-treatment with the mixed irreversible $MAO_{A/B}$ inhibitor, isocarboxazid caused no reduction in V_T (Supplemental Fig 2).

The global occupancy for each competition scan was calculated using the occupancy plot (*32*), (Fig. 5) and the resultant occupancy values were used to calculate the *in vivo* median effective dose (ED_{50}) of

idazoxan (Fig. 5 inset). Occupancy varied greatly between approximately 20% at 20 mg, and 80% at 80 mg, although for two individuals the occupancy was apparently negligible. The ED_{50} of idazoxan was calculated to be 0.27 mg·kg^{-1} and V_{ND} was estimated to be 19.2 ml·cm^{-3} (Fig. 5).

Test-Retest

Due to a technical failure of the well counter, blood data were not fully collected for one retest scan, thus test-retest data were only available from 5 subjects. *VAR* was reasonable, though quite high in several regions, above 10% in most subcortical and limbic regions. The ligand performs better throughout the cortex (Table 1; Supplemental Fig 3).

DISCUSSION

We present for the first time the characterisation of the novel imidazoline$_2$ binding site PET radioligand ^{11}C-BU99008 *in vivo* in humans. In this study, ^{11}C-BU99008 demonstrated a high specific signal in the brain, defined by blockade of the I_2BS by idazoxan along with reliable compartmental modelling and good selectivity.

There are some limitations on the competition study, including relatively low subject numbers and a restricted range of doses of idazoxan due to the upper limit on the tolerability of idazoxan (maximum dose 80 mg), and consequently the level to which the PET radioligand might be blocked. The limited dose range makes an estimation of the *in vivo* ED_{50} quite difficult, though it is encouraging to see such a clear dose-response over the range which we provided. The stability of occupancy measures at these doses is hard to estimate, but it should be noted that idazoxan had little effect in two subjects. This may be a case of differing metabolism of the drug; this could have been clarified by taking plasma concentration measurements but this option was not available during the study. In addition, these limitations make the nature of the idazoxan block difficult to determine. The reduction in V_T by the different doses of idazoxan

seen in Fig. 4 is not as obvious as might have been hoped. Some higher doses appear not to block as much of the ^{11}C-BU99008 binding as lower doses. One possible reason for this is a biphasic blockade by idazoxan. Unfortunately, the small numbers in this experiment do not allow this possibility to be fully explored. Considering these data in combination with the global occupancy, and generated dose response curve (Fig. 5) the simpler more conservative monophasic model of blockade is more appropriate.

There is some degree of variability, between 15 and 25% *VAR*, in outcome measure in subcortical regions, particularly the amygdala, striatum and other relatively high binding structures. This may be explained by the slow kinetics of the ligand consistent with a high V_T. We scanned for 2 hours, beyond which a carbon-11 label signal is no longer robust, so there is an indication that the kinetics will make the demonstration of group differences in subcortical ROIs difficult without large effect or group sizes. It is not, however, prohibitive, and the strong and robust cortical signal is very encouraging.

The lack of any reduction in signal following combined $MAO_{A/B}$ inhibition with isocarboxazid suggests ^{11}C-BU99008 has no significant off-target binding to MAO in humans. The idazoxan competition study gave a consistent V_{ND} of 19.2 ml·cm^{-3}, which represents about half of the total distribution volume in the lowest binding region (cerebellum), and less than 20% of the signal in the regions with highest binding. Thus, the specific signal is generally high throughout the brain with BP_{ND} values (estimated from the 2TCM as k_3/k_4) ranging from 1 to 4.

CONCLUSION

In summary, ^{11}C-BU99008 is able to image the I_2BS with high specificity and selectivity enabling the investigation of the function of I_2BS in the living human brain, along with disease states in which the I_2BS are known to be associated. The development of this new clinical imaging tool has hence paved the way for the conduct of more in-depth clinical investigations into the role of the I_2BS in disease states along with potential beneficial therapeutic intervention.

ACKNOWLEDGMENTS

The authors would like to thank Imanova Centre for Imaging Sciences for carrying out all PET syntheses and scans and providing logistical, technical and analytical support. This study was supported jointly by GSK and the MRC (MR/L01307X/1). We present independent research supported by the NIHR CRF at Imperial College Healthcare NHS Trust. The views expressed are those of the authors and not necessarily those of the MRC, the NHS, the NIHR or the Department of Health.

DISCLOSURE

This study was funded by the MRC (MR/L01307X/1) and GSK. No other potential conflicts of

REFERENCES

1. Regunathan S, Feinstein DL, Reis DJ. Expression of non-adrenergic imidazoline sites in rat cerebral cortical astrocytes. *J Neurosci Res.* 1993;34:681-688.

2. Morgan NG, Chan SL, Brown CA, Tsoli E. Characterization of the imidazoline binding site involved in regulation of insulin secretion. *Ann N Y Acad Sci.* 1995;763:361-373.

3. Finn DP, Marti O, Harbuz MS, et al. Behavioral, neuroendocrine and neurochemical effects of the imidazoline I2 receptor selective ligand BU224 in naive rats and rats exposed to the stress of the forced swim test. *Psychopharmacology (Berl).* 2003;167:195-202.

4. Garcia-Sevilla JA, Escriba PV, Sastre M, et al. Immunodetection and quantitation of imidazoline receptor proteins in platelets of patients with major depression and in brains of suicide victims. *Arch Gen Psychiatry.* 1996;53:803-810.

5. Sastre M, Ventayol P, Garcia-Sevilla JA. Decreased density of I2-imidazoline receptors in the postmortem brain of heroin addicts. *Neuroreport.* 1996;7:509-512.

6. Garcia-Sevilla JA, Escriba PV, Walzer C, Bouras C, Guimon J. Imidazoline receptor proteins in brains of patients with Alzheimer's disease. *Neurosci Lett.* 1998;247:95-98.

7. Reynolds GP, Boulton RM, Pearson SJ, Hudson AL, Nutt DJ. Imidazoline binding sites in Huntington's and Parkinson's disease putamen. *Eur J Pharmacol.* 1996;301:R19-21.

8. Ruiz-Durantez E, Torrecilla M, Pineda J, Ugedo L. Attenuation of acute and chronic effects of morphine by the imidazoline receptor ligand 2-(2-benzofuranyl)-2-imidazoline in rat locus coeruleus neurons. *Br J Pharmacol.* 2003;138:494-500.

9. Boronat MA, Olmos G, Garcia-Sevilla JA. Attenuation of tolerance to opioid-induced antinociception and protection against morphine-induced decrease of neurofilament proteins by idazoxan and other I2-imidazoline ligands. *Br J Pharmacol.* 1998;125:175-185.

10. Hudson AL, Gough R, Tyacke R, et al. Novel selective compounds for the investigation of imidazoline receptors. *Ann N Y Acad Sci.* 1999;881:81-91.

11. Casanovas A, Olmos G, Ribera J, Boronat MA, Esquerda JE, Garcia-Sevilla JA. Induction of reactive astrocytosis and prevention of motoneuron cell death by the I(2)-imidazoline receptor ligand LSL 60101. *Br J Pharmacol.* 2000;130:1767-1776.

12. Olmos G, Alemany R, Escriba PV, Garcia-Sevilla JA. The effects of chronic imidazoline drug treatment on glial fibrillary acidic protein concentrations in rat brain. *Br J Pharmacol.* 1994;111:997-1002.

13. Martin-Gomez JI, Ruiz J, Callado LF, et al. Increased density of I2-imidazoline receptors in human glioblastomas. *Neuroreport.* 1996;7:1393-1396.

14. Callado LF, Martin-Gomez JI, Ruiz J, Garibi JM, Meana JJ. Imidazoline I(2) receptor density increases with the malignancy of human gliomas. *J Neurol Neurosurg Psychiatry.* 2004;75:785-787.

15. Martin-Gomez JI, Ruiz J, Barrondo S, Callado LF, Meana JJ. Opposite changes in imidazoline I2 receptors and alpha2-adrenoceptors density in rat frontal cortex after induced gliosis. *Life Sci.* 2005;78:205-209.

16. Dardonville C, Rozas I. Imidazoline binding sites and their ligands: an overview of the different chemical structures. *Med Res Rev.* 2004;24:639-661.

17. Roeda D, Hinnen F, Dolle F. Radiosynthesis of a 2-substituted 4,5-dihydro-1H-[2-C-11] imidazole: the I-2 imidazoline receptor ligand [Cl-11 benazoline. *J Labelled Comp Radiopharm.* 2003;46:1141-1149.

18. Kawamura K, Kimura Y, Yui J, et al. PET study using [C-11]FTIMD with ultra-high specific activity to evaluate I-2-imidazoline receptors binding in rat brains. *Nucl Med Biol.* 2012;39:199-206.

19. Kawamura K, Naganawa M, Konno F, et al. Imaging of I-2-imidazoline receptors by small-animal PET using 2-(3-fluoro-[4-C-11]tolyl)-4,5-dihydro-1H-imidazole ([C-11]FTIMD). *Nucl Med Biol.* 2010;37:625-635.

20. Kealey S, Turner EM, Husbands SM, et al. Imaging imidazoline-I2 binding sites in porcine brain using 11C-BU99008. *J Nucl Med.* 2013;54:139-144.

21. Parker CA, Nabulsi N, Holden D, et al. Evaluation of 11C-BU99008, a PET Ligand for the Imidazoline2 Binding Sites in Rhesus Brain. *J Nucl Med.* 2014;55:838-844.

22. Tyacke RJ, Fisher A, Robinson ES, et al. Evaluation and initial in vitro and ex vivo characterization of the potential positron emission tomography ligand, BU99008 (2-(4,5-dihydro-1H-imidazol-2-yl)-1-methyl-1H-indole), for the imidazoline(2) binding site. *Synapse.* 2012;66:542-551.

23. Litman RE, Su TP, Potter WZ, Hong WW, Pickar D. Idazoxan and response to typical neuroleptics in treatment-resistant schizophrenia. Comparison with the atypical neuroleptic, clozapine. *Br J Psychiatry.* 1996;168:571-579.

24. Osman OT, Rudorfer MV, Potter WZ. Idazoxan: a selective alpha 2-antagonist and effective sustained antidepressant in two bipolar depressed patients. *Arch Gen Psychiatry.* 1989;46:958-959.

25. De Vos H, Convents A, De Keyser J, et al. Autoradiographic distribution of alpha 2 adrenoceptors, NAIBS, and 5-HT1A receptors in human brain using [3H]idazoxan and [3H]rauwolscine. *Brain Res.* 1991;566:13-20.

26. De Vos H, Bricca G, De Keyser J, De Backer JP, Bousquet P, Vauquelin G. Imidazoline receptors, non-adrenergic idazoxan binding sites and alpha 2-adrenoceptors in the human central nervous system. *Neuroscience.* 1994;59:589-598.

27. Davidson J, Turnbull C. Isocarboxazid. Efficacy and tolerance. *J Affect Disord.* 1983;5:183-189.

28. Eglen RM, Hudson AL, Kendall DA, et al. 'Seeing through a glass darkly': casting light on imidazoline 'I' sites. *Trends Pharmacol Sci.* 1998;19:381-390.

29. Alemany R, Olmos G, Garcia-Sevilla JA. The effects of phenelzine and other monoamine oxidase inhibitor antidepressants on brain and liver I2 imidazoline-preferring receptors. *Br J Pharmacol.* 1995;114:837-845.

30. Tziortzi AC, Searle GE, Tzimopoulou S, et al. Imaging dopamine receptors in humans with [11C]-(+)-PHNO: dissection of D3 signal and anatomy. *Neuroimage.* 2011;54:264-277.

31. Ichise M, Toyama H, Innis RB, Carson RE. Strategies to improve neuroreceptor parameter estimation by linear regression analysis. *J Cereb Blood Flow Metab.* 2002;22:1271-1281.

32. Cunningham VJ, Rabiner EA, Slifstein M, Laruelle M, Gunn RN. Measuring drug occupancy in the absence of a reference region: the Lassen plot re-visited. *J Cereb Blood Flow Metab.* 2010;30:46-50.

FIGURES AND TABLES

Region	V_T ± SD (mL·cm^{-3})			AIC		*VAR*		
	1TCM	2TCM	MA1	1TCM	2TCM	1TCM	2TCM	MA1
Whole Brain	44.5 ± 6.1	48.8 ± 7.9	44.8 ± 6.1	-237	-328	12.9	6.4	13.4
Cerebellum	39.3 ± 6.2	41.9 ± 6.9	39.6 ± 6.2	-237	-310	14.6	10.8	14.9
Brain Stem	62.7 ± 9.1	66.4 ± 10.1	63.2 ± 9.2	-252	-276	13.7	11.7	14.6
Occipital Lobe	38.6 ± 6.5	42.7 ± 8.6	38.8 ± 6.5	-234	-323	12.8	8.1	13.3
Insula	63.3 ± 9.0	67.7 ± 11.8	63.9 ± 9.1	-224	-267	14.6	11.0	14.8
Frontal Lobe	41.6 ± 5.9	45.7 ± 7.9	42.0 ± 5.9	-225	-316	12.6	4.7	13.1
Cingulate	58.3 ± 8.6	62.2 ± 9.7	58.8 ± 8.6	-222	-293	14.6	10.2	15.1
Parietal Lobe	39.2 ± 5.8	43.6 ± 8.7	39.5 ± 5.9	-233	-318	12.4	5.6	12.8
Amygdala	89.8 ± 15.2	94.6 ± 20.3	91.1 ± 15.1	-233	-242	23.2	24.7	23.3
Hippocampus	68.4 ± 11.4	77.7 ± 24.2	69.1 ± 11.5	-225	-264	16.1	15.9	16.4
Striatum	102.7 ± 17.8	105.7 ± 21.0	104.2 ± 17.6	-246	-259	16.9	16.7	17.4
Thalamus	75.3 ± 11.0	80.0 ± 14.1	76.0 ± 11.1	-228	-264	14.6	9.5	15.2

TABLE 1. Outcome measures for selected regions of interest from three models one-tissue (1TCM) and two-tissue (2TCM) compartmental models with fixed blood volume (5%) and MA1, including volume of distribution (V_T), the goodness-of-fit parameter the Akaike Information Criterion (AIC) and the test-retest variability (*VAR*). For V_T and AIC, the complete baseline dataset is presented (n=14), for *VAR*, the test-retest cohort (n=5).

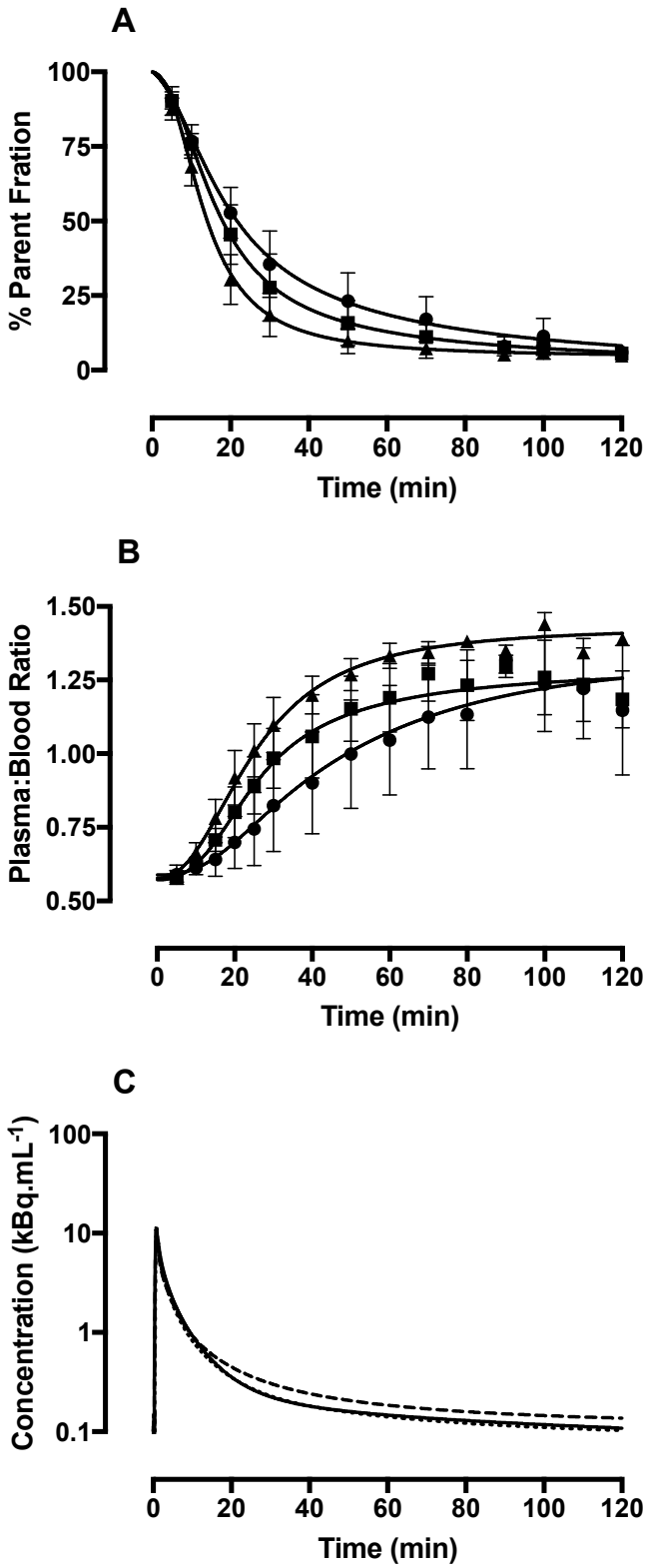

FIGURE 1. The mean fits for parent fraction (A, sigmoid), plasma:blood (B,sigmoid) for unblocked scans (circles), Idazoxan blocked scans (squares) and Isocarboxazid scans (triangle). Vertical bars represent the standard deviation. Panel C is the calculated parent plasma input function (C, tri-exponential) for unblocked scans (solid line), Idazoxan blocked scans (dashed line) and Isocarboxazid scans (dotted line).

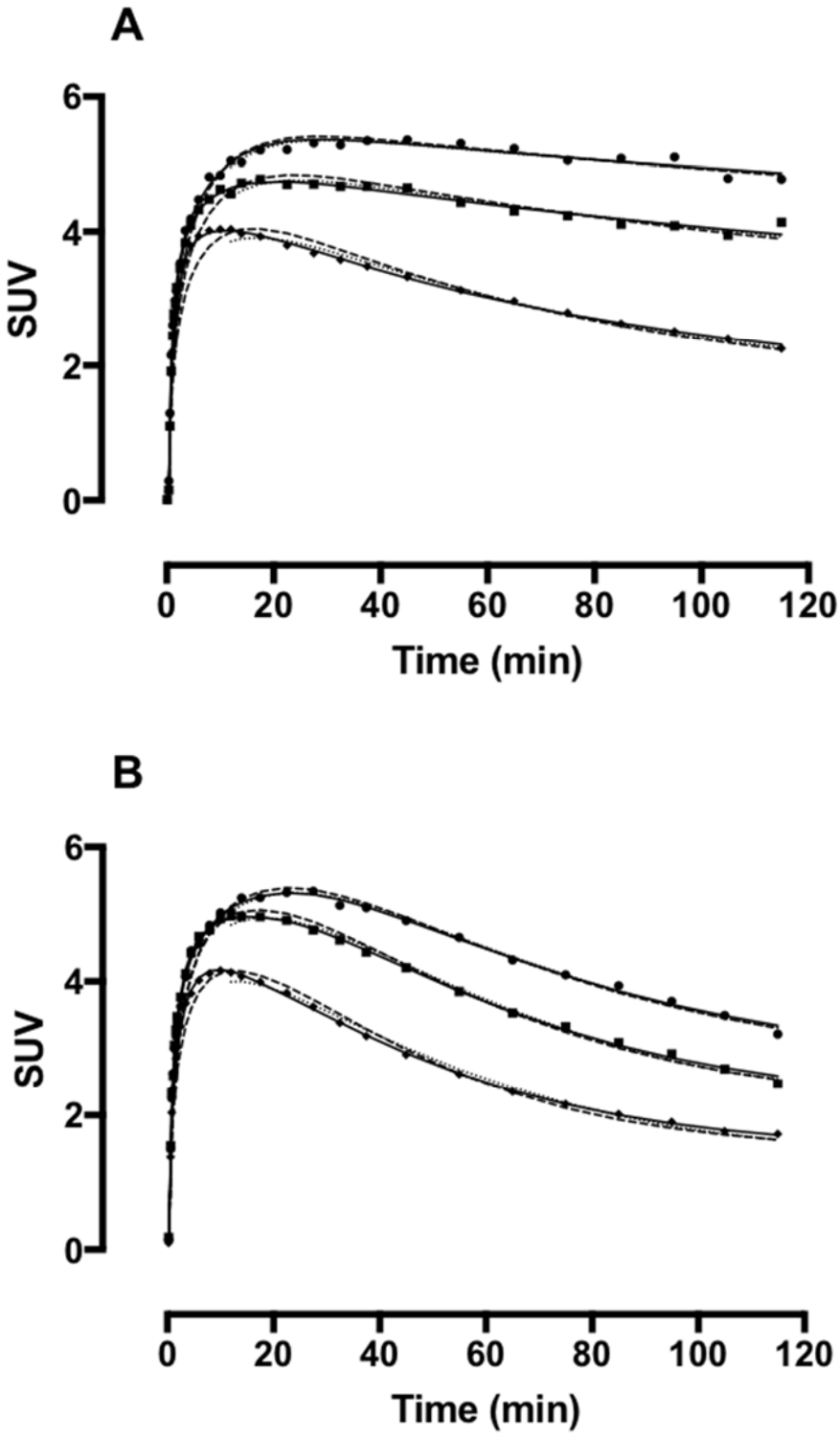

FIGURE 2. Representative TACs for [11]C-BU99008 uptake into human brain at baseline (A), and partially blocked (B) after participant was treated with Idazoxan (80 mg). ROIs – striatum (circles); thalamus (squares); cerebellum (diamond). The fitted lines are derived from the 3 main models tested – 1TCM, dashed line; 2TCM, solid line; MA1, dotted line.

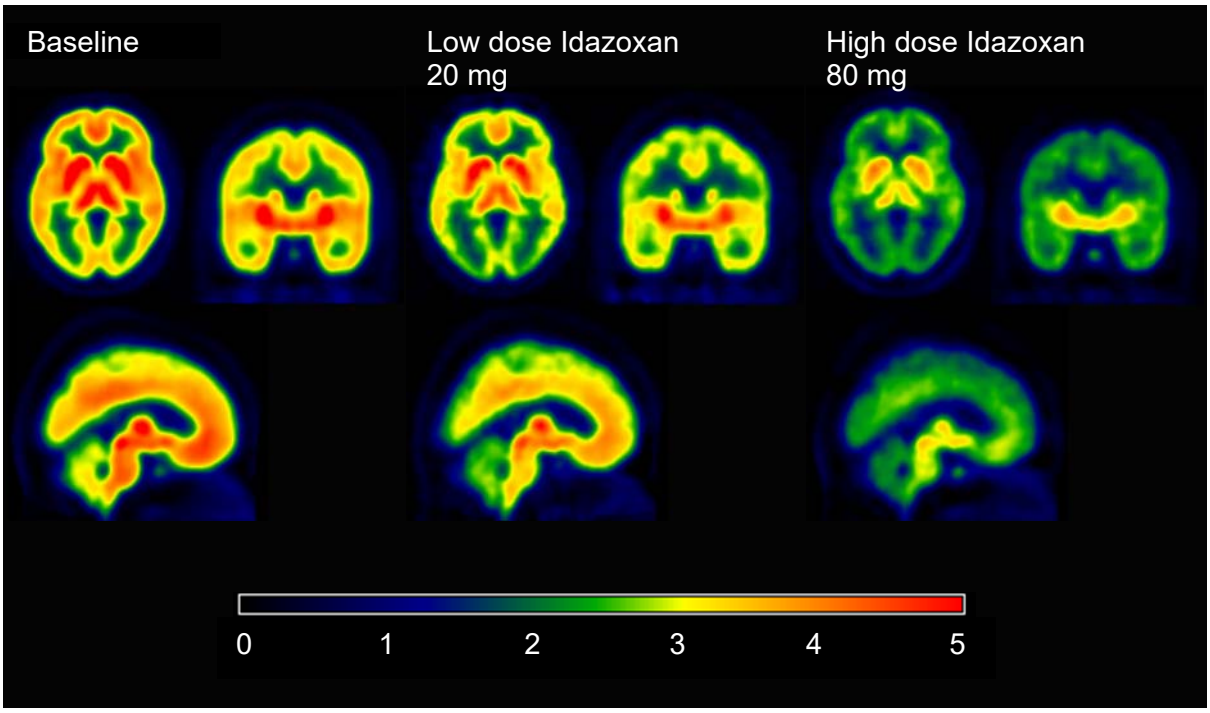

FIGURE 3. SUV images to demonstrate brain heterogeneous brain uptake in all regions and a dose-dependent blockade by idazoxan.

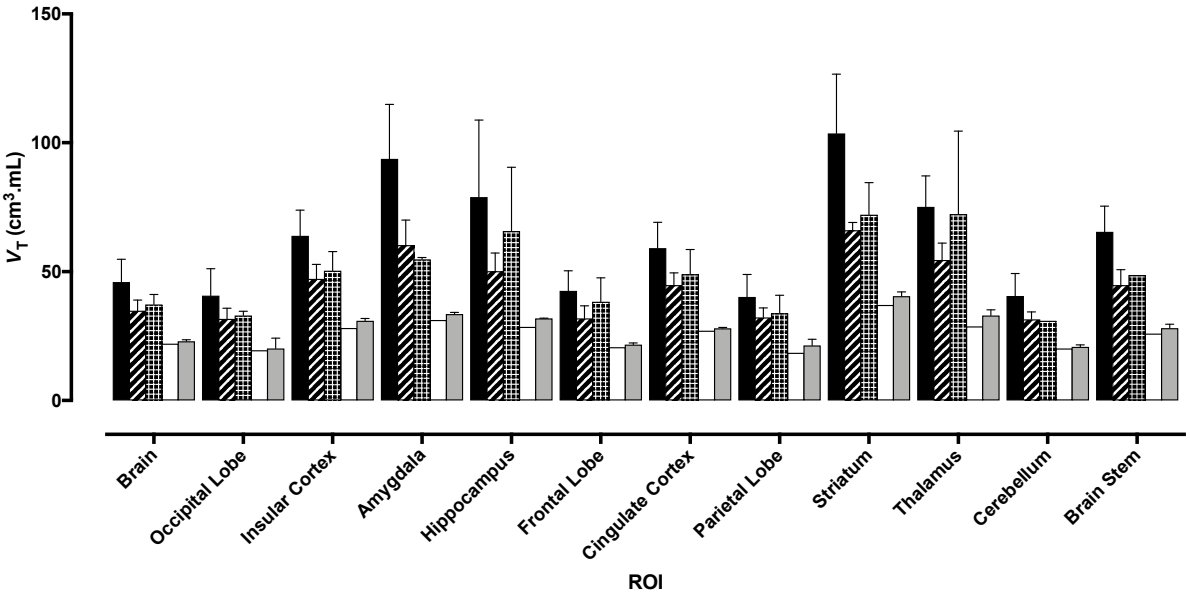

FIGURE 4. Bar chart showing regional distribution volume (V_T) of ^{11}C-BU99008 and effect of increasing doses of the mixed I_2BS/α_2-adrenoceptor ligand Idazoxan: 20 mg (striped), 40 mg (checkered), 60 mg (clear), 80 mg (grey), and baseline (black). Bars represent mean ± SD. Data from a selection of representative brain regions.

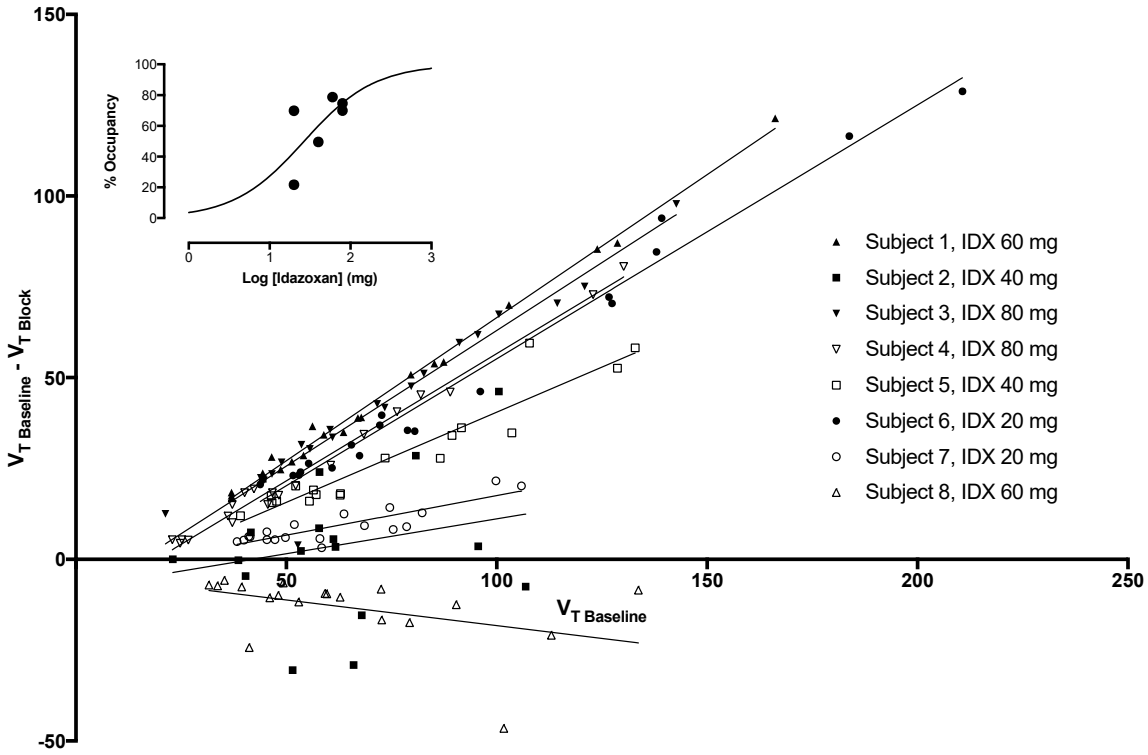

FIGURE 5. Occupancy plots for the n=8 subjects in the heterologous block study. A dose-response curve for those individuals where occupancy was observed is included (inset). The ED_{50} was calculated to be 27.7 mg or 0.27 mg·kg^{-1}, and the V_{ND} estimated to be 19.2.